IEEE Access
Multidisciplinary | Rapid Review | Open Access Journal

Received May 21, 2019, accepted June 4, 2019, date of publication June 17, 2019, date of current version July 10, 2019.

Digital Object Identifier 10.1109/ACCESS.2019.2923458

Energy Management and Control Strategy of Photovoltaic/Battery Hybrid Distributed Power Generation Systems With an Integrated Three-Port Power Converter

JIATU HONG[1], JIAN YIN[1], (Member, IEEE), YITAO LIU[1], (Member, IEEE), JIANCHUN PENG[1], (Senior Member, IEEE), AND HUI JIANG[2]

[1]College of Mechatronics and Control Engineering, Shenzhen University, Shenzhen 518060, China
[2]College of Optoelectronic Engineering, Shenzhen University, Shenzhen 518060, China

Corresponding author: Jian Yin (jyin@szu.edu.cn)

This work was supported in part by the National Natural Science Foundation of China under Grant 51707124, in part by the Foundation for Distinguished Young Talents in Higher Education of Guangdong China under Grant 2016KQNCX148, in part by the Natural Science Foundation of Guangdong Province under Grant 2016A030313041, in part by the Shenzhen Science and Technology Research Foundation for Basic Project under Grant JCYJ20170302153607971, and in part by the Shenzhen Peacock Program under Grant 827/000237.

ABSTRACT Photovoltaic (PV)/battery hybrid power units have attracted vast research interests in recent years. For the conventional distributed power generation systems with PV/battery hybrid power units, two independent power converters, including a unidirectional dc–dc converter and a bidirectional converter, are normally required. This paper proposes an energy management and control strategy for the PV/battery hybrid distributed power generation systems with only one integrated three-port power converter. As the integrated bidirectional converter shares power switches with the full-bridge dc–dc converter, the power density and the reliability of the system is enhanced. The corresponding energy management and control strategy are proposed to realize the power balance among three ports in different operating scenarios, which comprehensively takes both the maximum power point tracking (MPPT) benefit and the battery charging/discharging management into consideration. The simulations are conducted using the Matlab/Simulink software to verify the operation performance of the proposed PV/battery hybrid distributed power generation system with the corresponding control algorithms, where the MPPT control loop, the battery charging/discharging management loop are enabled accordingly in different operating scenarios.

INDEX TERMS Energy management, maximum power point tracking, bidirectional power converter, photovoltaic/battery hybrid power unit.

I. INTRODUCTION

With the development of the power electronic technology, a larger amount of PV panels are integrated as power sources into the distributed power generation systems [1], [2]. For example, renewable energy consumption (excluding hydro) of the world grew by 17% in 2017, and the solar energy contributed more than a third of the total renewables growth despite accounting for just 21% of the total renewables power generation [3]. The energy storage system (ESS) technology is undoubtedly the key solution to the intermittent nature of the renewable energy sources [4]–[6].

A PV/battery hybrid power unit forms the most basic topology among various distributed power generation systems. Normally the conventional PV/battery hybrid power unit based on the DC/AC microgrids includes at least two independent power converters with a unidirectional DC-DC conversion stage and a bidirectional conversion stage [7]–[12], which is shown in Fig. 1 (a) (the DC microgrid based system for example). The unidirectional DC-DC converter interfaces the PV with the DC bus, and the bidirectional converter interfaces the ESS such as the battery with the DC bus. Literatures focus on the improvement of

The associate editor coordinating the review of this manuscript and approving it for publication was Yang Han.

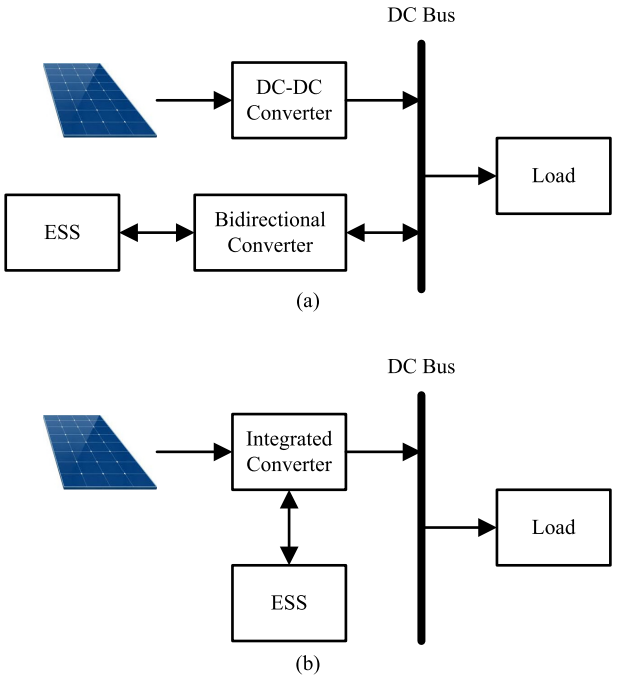

FIGURE 1. (a) Conventional topology for the PV/battery hybrid power unit with two independent power converters; (b) Proposed topology for the PV/battery hybrid power unit with an integrated three-port power converter.

the control and power management scheme based on the DC/AC hybrid microgrids, AC microgrid and DC microgrid, either in the grid-connected or the islanded operating mode [7]–[10]. Some literatures focus on the application of the PV/battery hybrid power system based on the DC microgrid alone [11]. Normally, a comprehensive control strategy for the PV/battery hybrid power system incorporates the PV array controller for MPPT purpose, the battery controller for charging/discharging management and state of charge (SOC) control purpose, the inverter controller (for the system based on the AC microgrid) [7]. In addition, the application of the battery/supercapacitor hybrid energy storage unit in the PV based distributed power generation system has been discussed in [11] and [12].

Compared with the conventional topology, an integrated three-port power converter as the interface for the PV/battery hybrid power generation system is shown in Fig. 1 (b). The two independent converters of the conventional topology in Fig. 1 (a) are combined and therefore the power density of the system can be enhanced. The concept, modeling and design of the multiport power converters for interfacing renewable power sources and energy storage units are introduced in [13]. Authors pointed out that the reliability and dynamic response of the conventional multi-converter topology can be compromised since such discrete system requires coordinated control on the power flow and load regulation through the communication channel. The multiport converter interfacing the power source, battery and load can be derived by using the multi-winding transformer [14], [15], either based on the full-bridge module or the half-bridge module. However, this kind of multi-winding transformer based multiport converter may require a large number of power switches which reduces the power density and meanwhile increases the cost and the complexity of driving and control. A hybrid PV-wind-battery-load four-port distributed power generation system is proposed in [16]. The proposed four-port topology is derived by simply adding two power switches based on the conventional half-bridge converter, and therefore high power density of the system is achieved. The concept of the boost-integrated phase shift full-bridge three-port converter is proposed in [17]. Two boost-integrated three-port converter topologies, namely the symmetric and asymmetric topologies are presented for potential applications of the PV/fuel cells based distributed power generation systems. By regulating the duty cycle of power switches, bidirectional power flow can be achieved between the two ports at the primary side of the high-frequency (HF) transformer. Compared with the equivalent conventional system, the utilization of the integrated topologies benefits the system in terms of higher efficiency, higher power density and decreased cost.

An integrated three-port DC-DC converter combining an interleaved bidirectional buck–boost converter and a phase-shift full-bridge converter for the PV/battery hybrid power generation system is proposed based on the concept of the symmetric boost-integrated three-port topology [18]. The proposed PWM plus phase angle shift control scheme is verified as a suitable candidate for the PV/battery hybrid three-port power generation system. In addition, the possibility of the topology extension to derive converters with four or more ports is discussed.

Compared with the symmetric boost-integrated three-port topology, a DC blocking capacitor in the HF link is indispensable for the asymmetric topology as the average voltage difference between midpoints of the two switching legs appears in this case. Based on the concept of the asymmetric topology for the boost-integrated full-bridge converter, this paper investigates its potential application performance in the DC microgrid based PV/battery hybrid power unit with an integrated three-port power converter. In addition, a corresponding energy management and control strategy is proposed to achieve the automatic energy management and optimal system performance. Potential operating scenarios of the system under various power conditions are presented in detail. Simulations are conducted to verify the feasibility of the PV/battery hybrid power generation system with the proposed energy management and control strategy.

II. BASIC ANALYSIS

The proposed PV/battery hybrid distributed power generation system is shown in Fig. 2. This is a three-port system interfacing a PV, an ESS unit (a battery for example) and a DC load. The battery serves as an energy buffer, which means it can be charged or discharged to balance the power flow in the PV/battery hybrid power system. As shown in Fig. 2, the phase-shift full-bridge DC-DC converter interfacing the PV and the load shares power switches with the integrated

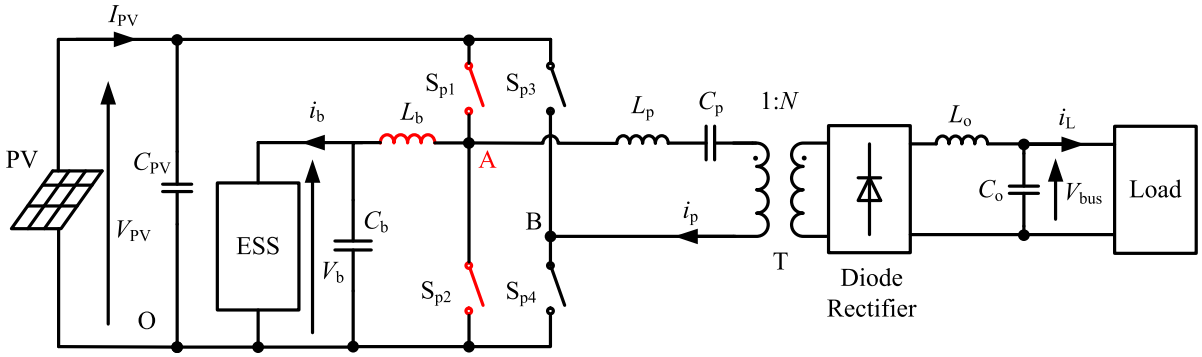

FIGURE 2. The proposed PV/battery hybrid distributed power generation system.

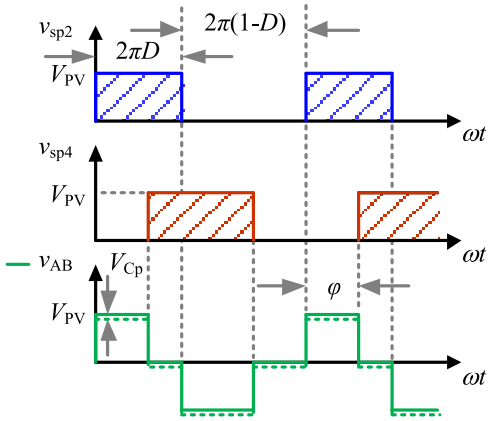

FIGURE 3. Modulation strategy of the full bridge with the phase shift angle φ and the duty cycle D.

bidirectional buck/boost converter interfacing the battery, based on which the power density of the system is enhanced compared with the conventional topology consisting of the independent phase-shift full-bridge DC-DC converter and bidirectional converter.

A modified phase-shift modulation scheme is adopted for the primary full bridge as shown in Fig. 3. Two switching legs of the primary full bridge are phase shifted by the angle φ. In addition, the duty cycle of switches S_{p1} and S_{p2} on leg A can be regulated, while the duty cycle of the other two switches is fixed at 50%.

The integrated bidirectional buck/boost converter interfacing the battery at the primary side of the HF transformer is highlighted in Fig. 2. The battery, capacitor C_b, inductor L_b, two power switches of the leg A and the PV side bus form a bidirectional buck/boost topology inherently. When the battery is charged with $i_b > 0$, the topology operates in the buck mode. When the battery is discharged with $i_b < 0$, then the topology operates in the boost mode. Therefore, the bidirectional power flow can be achieved for the battery with the charging/discharging management requirement.

According to the buck/boost operating principle, since the battery voltage V_b can be considered as almost constant during the normal SOC period, the PV output voltage V_{PV} can be regulated to achieve MPPT by control of the duty cycle D.

Assuming that the inductor L_b is large enough, V_{PV} is derived as

$$V_{PV} = V_b/D \tag{1}$$

where D represents the duty cycle of the switch S_{p1} of leg A as shown in Fig. 3. In addition, the phase shift angle φ is adopted as another control variable to obtain the required DC bus voltage V_{bus}. Due to the asymmetric modulation with two legs of the full bridge, v_{AB} contains a DC component, which can compromise the normal operation of the HF transformer. In this paper, a DC blocking capacitor C_p is incorporated to prevent the HF transformer from saturation. According to the volt-second balance principle for the inductor L_p and the HF transformer, the DC blocking capacitor C_p voltage V_{Cp} is derived as

$$V_{Cp} = V_{PV}\left(D - \frac{1}{2}\right) \tag{2}$$

Based on the volt-second balance principle for the inductor L_o and assuming L_o is large enough, the DC bus voltage V_{bus} can be expressed as

$$V_{bus} = N\left\{\frac{\varphi}{2\pi}(V_{PV}-V_{Cp})+\left(\frac{1}{2}+\frac{\varphi}{2\pi}-D\right)(V_{PV}+V_{Cp}) + \left[1-\left(\frac{1}{2}+\frac{\varphi}{2\pi}-D+\frac{\varphi}{2\pi}\right)\right]|V_{Cp}|\right\} \tag{3}$$

where the turns ratio of the transformer is defined as 1:N. Then the DC bus voltage V_{bus} can be derived as

$$V_{bus} = \begin{cases} NV_{PV}\dfrac{\varphi}{\pi}\left(\dfrac{3}{2}-D\right), & D > \dfrac{1}{2} \\ NV_{PV}\left[\dfrac{\varphi}{\pi}\left(\dfrac{1}{2}+D\right)+\dfrac{1}{2}-2D^2\right], & D < \dfrac{1}{2}. \end{cases} \tag{4}$$

According to Fig. 3, the following constraints need to be applied for the modulation scheme as

$$\begin{cases} D > \dfrac{\varphi}{2\pi} \\ \dfrac{1}{2}+\dfrac{\varphi}{2\pi}-D > 0 \end{cases} \tag{5}$$

which can be further derived as

$$\frac{\varphi}{2\pi} < D < \frac{\varphi}{2\pi}+\frac{1}{2} \tag{6}$$

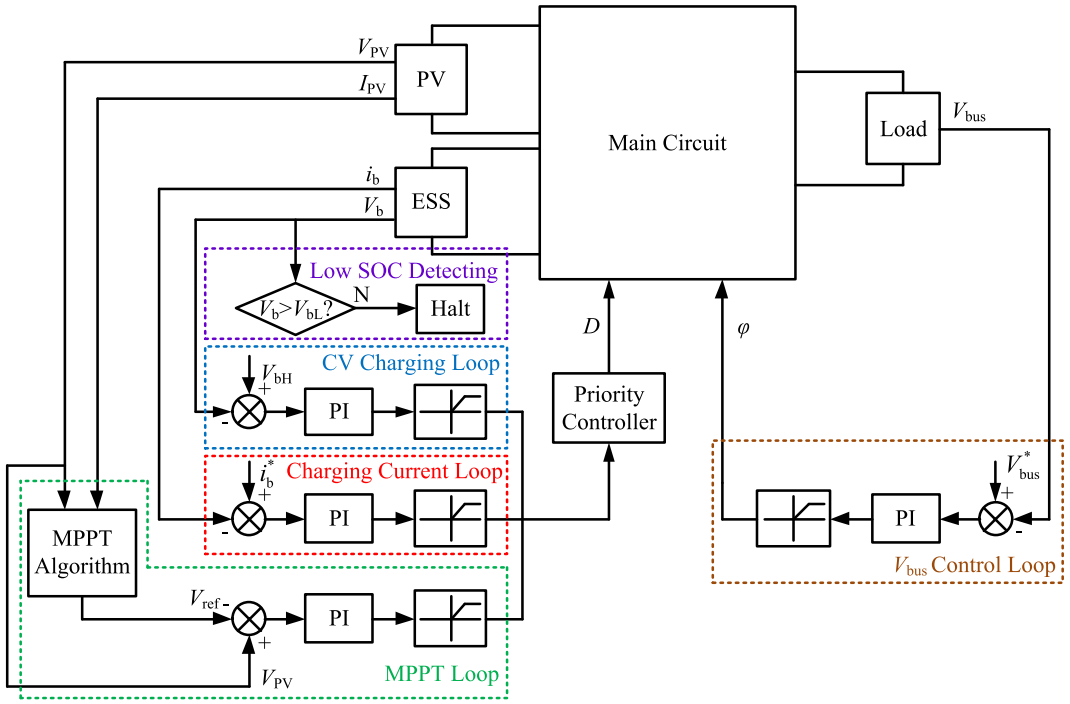

FIGURE 4. Control algorithm of the proposed PV/battery hybrid distributed power generation system.

φ and D serve as the only two control variables for the proposed PV/battery hybrid distributed power generation system, based on which a corresponding energy management and control strategy is proposed in the following section.

III. CONTROL ALGORITHM

The control algorithm of the proposed PV/battery hybrid distributed power generation system is shown in Fig. 4. Various MPPT techniques have been introduced in [19]. In this paper, only the conventional incremental conductance MPPT technique is adopted since the improvement of the MPPT algorism is not the focus of this paper.

As shown in Fig. 4, the phase shift angle φ of the full bridge is used to control the load side DC bus voltage V_{bus} through a PI controller. The PV reference voltage V_{ref} is obtained by the basic incremental conductance MPPT algorithm. In addition, a low SOC detecting part is incorporated in the control system to temporarily halt the operation of the system (such as setting the phase shift angle φ as zero) when the battery voltage V_b drops to a low value V_{bL}.

The duty cycle D serves as the key control variable to achieve the power balance and automatic control in different operation scenarios of the whole power generation system. There are three control loops competing to take charge of the duty cycle D, namely the constant voltage (CV) charging loop, charging current loop and MPPT loop. The priority controller determines which control loop to enable. The overall objective is to achieve the power balance of the whole power system and automatic battery charging/discharging management, while have the PV to operate at the maximum power point if possible. In this paper, the priority controller is to obtain the minimum value among three control loop outputs.

For example, when the load power P_L is larger than the PV maximum output power P_{MPP} but within the most power that the PV and battery can supply in combination, the battery would operate in the discharging mode, and therefore the battery charging current i_b would turn negative, which results in the saturation for the output of the charging current loop. Then in this case the MPPT control loop would be enabled (assuming the battery voltage V_b is lower than the CV charging voltage V_{bH} and the CV charging loop is disabled), and the duty cycle D would be regulated until the PV operates near the maximum power point. It is noted that the battery serves as a power balance port in this case.

When the load power is relatively small, there can be much surplus power from the PV supposing the MPPT control loop is enabled, which can cause high battery charging power beyond the specific battery charging requirements. In this case the input error signal of the charging current control loop would turn negative, which means the corresponding loop would take charge over the duty cycle D (assuming the battery voltage V_b is lower than the CV charging voltage V_{bH} and the CV charging loop is disabled). Therefore the battery would operate in the constant current (CC) charging mode at a preset level of i_b^*. It is noted that the PV serves as a power balance port in this case and the operating point of the PV would be regulated accordingly to achieve the power balance of the system.

For the CV charging loop, when the battery voltage V_b reaches the preset CV charging voltage V_{bH}, the CV charging loop is enabled and the battery would operate in the CV

charging mode. Since the charging power is unstable and uncontrollable for the CV charging mode, the operating point of the PV would change through the CV charging process to achieve the power balance.

Potential operation scenarios of the proposed PV/battery hybrid distributed power generation system under various power conditions among three ports are illustrated below as scenario 1 to scenario 7.

1) Scenario 1: The load power is larger than the most power that the PV and battery can supply in combination. In this case either the whole system needs to be halted, or measures such as the load shedding needs to be taken.
2) Scenario 2: The load power is larger than the PV maximum output power P_{MPP}, but within the most power that the PV and battery can supply in combination. In this case the MPPT control loop would be enabled to utilize the most of the solar energy under the specific irradiance and temperature conditions. In the meantime, the battery would operate in the discharging mode and supply a part of the load power, which achieves the power balance for the system.
3) Scenario 3: The PV maximum power P_{MPP} just equals to the load power. In this case the battery would not be charged or discharged and the PV supplies the load power solely at the maximum power point.
4) Scenario 4: The PV maximum power P_{MPP} is larger than the load power, and the surplus power from the PV is within the maximum charging power of the battery. In this case, the MPPT control loop would be enabled and the PV would supply the load and charge the battery in the meantime. The battery serves as the power balance port of the system in this case.
5) Scenario 5: The PV maximum power P_{MPP} is larger than the total of the load power and the maximum charging power of the battery under the specific irradiance and temperature conditions. In this conditions. In this case the battery charging current i_{b} control loop would be enabled and the MPPT control loop would be disabled. The battery would operate in the constant current charging mode at a preset level of i_{b}^{*}. In the meantime, the operating point of the PV would be regulated accordingly until the power balance of the system can be achieved.
6) Scenario 6: The PV output power is near zero (for example in the evening) and the load power is larger than the maximum discharging power of the battery. In this case either the whole system needs to be halted, or measures such as the load shedding needs to be taken.
7) Scenario 7: The PV output power is near zero and the load power is within the maximum discharging power of the battery. In this case the battery would operate in the discharging mode as the only power source.

A brief illustration about different potential operation scenarios mentioned above is shown in Table 1. $P_{\mathrm{DCHG}}^{\mathrm{Max}}$ represents the maximum discharging power of the battery and $P_{\mathrm{CHG}}^{\mathrm{Max}}$ represents the maximum charging power of the battery, and both are determined by the specific application requirements of the battery. In addition, a flow diagram of the proposed control algorithm is presented in Fig. 5.

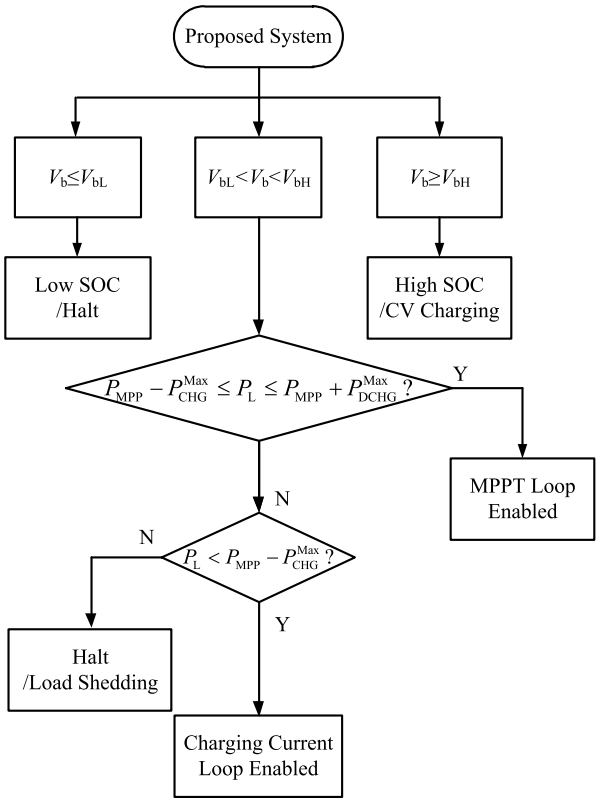

FIGURE 5. Flow diagram of the proposed control algorithm.

TABLE 1. Operation scenarios of the system.

Scenarios	Power Conditions	MPPT
1	$P_{\mathrm{L}} > P_{\mathrm{MPP}} + P_{\mathrm{DCHG}}^{\mathrm{Max}}$	-
2	$P_{\mathrm{MPP}} < P_{\mathrm{L}} \le P_{\mathrm{MPP}} + P_{\mathrm{DCHG}}^{\mathrm{Max}}$	Enabled
3	$P_{\mathrm{L}} = P_{\mathrm{MPP}}$	Enabled
4	$P_{\mathrm{MPP}} - P_{\mathrm{CHG}}^{\mathrm{Max}} \le P_{\mathrm{L}} < P_{\mathrm{MPP}}$	Enabled
5	$P_{\mathrm{L}} < P_{\mathrm{MPP}} - P_{\mathrm{CHG}}^{\mathrm{Max}}$	-
6	$P_{\mathrm{PV}} = 0$, $P_{\mathrm{L}} > P_{\mathrm{DCHG}}^{\mathrm{Max}}$	-
7	$P_{\mathrm{PV}} = 0$, $P_{\mathrm{L}} \le P_{\mathrm{DCHG}}^{\mathrm{Max}}$	-

IV. SIMULATION RESULTS

The simulations of the proposed PV/battery hybrid distributed power generation system are conducted using the Matlab/Simulink software. The PV array model is built of strings of PV modules connected in parallel and each string consists of modules connected in series. The PV module model used in this paper is based on the PV module 1STH-215-P of the 1Soltech company according to the National Renewable Energy Laboratory (NREL) System

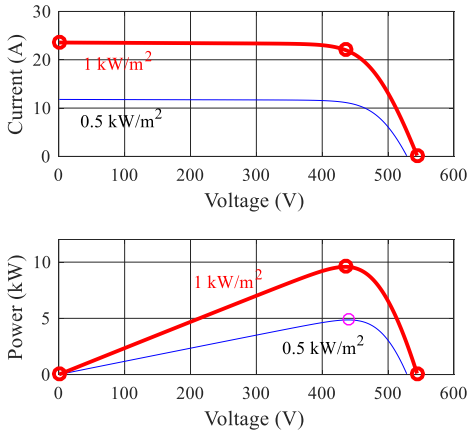

FIGURE 6. PV characteristic curves with Irradiance = 1 kW/m^2 (red) and Irradiance = 0.5 kW/m^2 (blue) (Temperature = 25°C).

TABLE 2. Parameters of the matlab/simulink model.

Parameters	Values
PV Maximum Power P_{MPP} (1000 W/m^2)	9.6 kW
Maximum Power Point Voltage V_{MPP} (1000 W/m^2)	435 V
Maximum Power Point Current I_{MPP} (1000 W/m^2)	22 A
PV Maximum Power P_{MPP} (500 W/m^2)	4.9 kW
Maximum Power Point Voltage V_{MPP} (500 W/m^2)	440 V
Maximum Power Point Current I_{MPP} (500 W/m^2)	11 A
Nominal DC Bus Voltage V_{bus}^*	500 V
Battery Nominal Voltage V_b	200 V
Battery Maximum Charged Voltage V_{bH}	208 V
Battery Maximum Charge/Discharge Current	30 A
Switching Frequency f_{sw}	20 kHz
Inductor L_p	45 µH
Capacitor C_p	2 µF
Inductor L_b	1.5 mH
Transformer Turns Ratio 1:N	2:3

Advisory Model database. PV characteristic curves with Irradiance = 1 kW/m^2 and 0.5 kW/m^2 (Temperature = 25 °C) are shown in Fig. 6. The ideal values of the maximum power point for the PV characteristic curve under standard test conditions (STC) (Irradiance = 1 kW/m^2, Temperature = 25 °C) are as follows: $V_{MPP} = 435$ V, $I_{MPP} = 22$ A, $P_{MPP} \approx 9.6$ kW. The main simulation parameters are shown in Table 2. Both the steady state and dynamic response simulation results are presented below.

A. STEADY STATE SIMULATION RESULTS

1) SCENARIO 2

The steady state simulation results of the operation scenario 2 are shown in Fig. 7. The simulation conditions are as follows: Irradiance = 1000 W/m^2, Temperature = 25 °C), the load power $P_L = 10$ kW. By regulating the phase shift

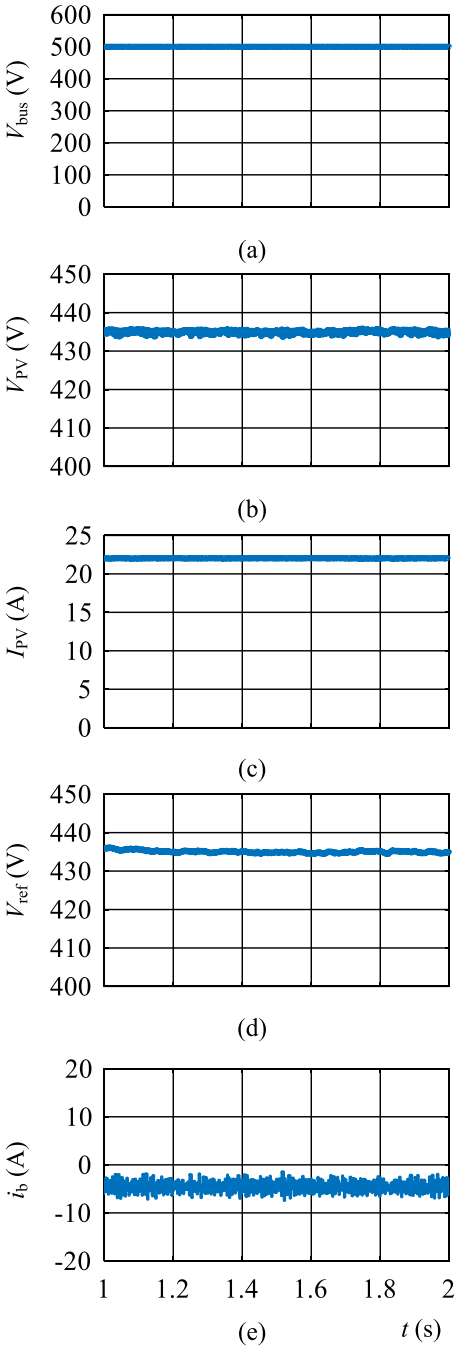

FIGURE 7. Steady state simulation results of operation scenario 2. (a) DC bus voltage V_{bus}; (b) PV voltage V_{PV}; (c) PV current I_{PV}; (d) PV reference voltage V_{ref}; (e) Battery charging current i_b.

angle φ through a PI controller, the DC bus voltage V_{bus} is controlled at the preset value $V_{bus}^* = 500$ V, which is shown in Fig. 7 (a). From Fig. 7 (b), Fig. 7 (c) and Fig. 7 (d), since the MPPT loop is enabled in this scenario, the PV operates at the maximum power point with V_{PV} controlled near the ideal value $V_{MPP} = 435$ V and I_{PV} controlled near the ideal value $I_{MPP} = 22$ A. According to Fig. 7 (e), the battery operates in the discharging mode and supplies a part of the load power in this scenario.

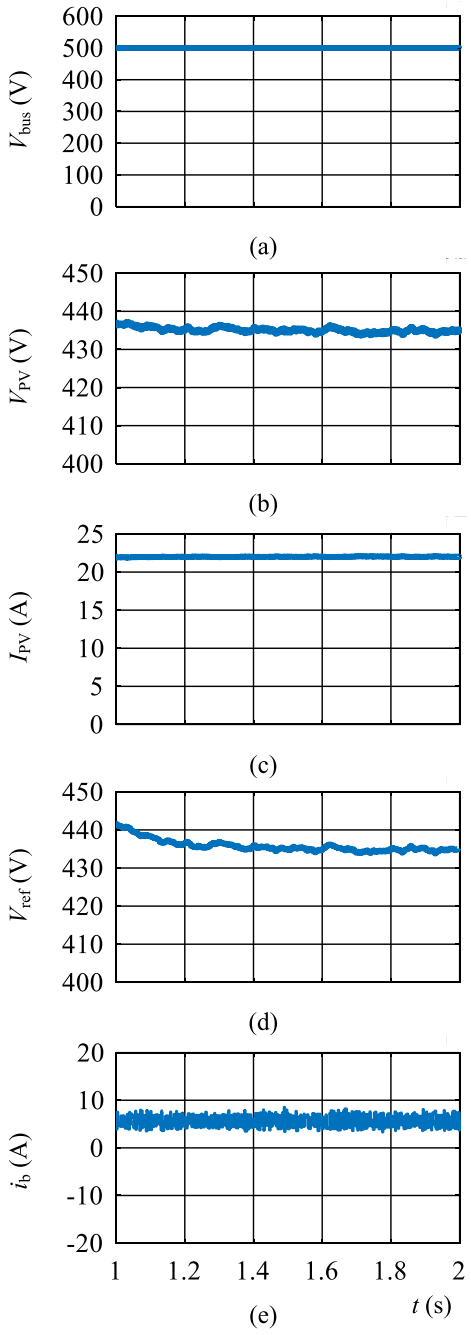

FIGURE 8. Steady state simulation results of operation scenario 4. (a) DC bus voltage V_{bus}; (b) PV voltage V_{PV}; (c) PV current I_{PV}; (d) PV reference voltage V_{ref}; (e) Battery charging current i_b.

2) SCENARIO 4

The steady state simulation results of the operation scenario 4 are shown in Fig. 8. The simulation conditions are as follows: Irradiance = 1000 W/m^2, Temperature = 25°C), the load power $P_L = 8$ kW. The DC bus voltage V_{bus} is controlled at the preset value $V^*_{bus} = 500$ V as shown in Fig. 8(a). From Fig. 8 (b), Fig. 8 (c) and Fig. 8 (d), the MPPT loop is also enabled in this scenario and the PV operates at the maximum power point with V_{PV} controlled near the ideal value $V_{MPP} = 435$ V and I_{PV} controlled near the ideal value $I_{MPP} = 22$ A. According to Fig. 8 (e), the battery operates in the charging mode in this scenario and the surplus power from the PV can be stored in the battery.

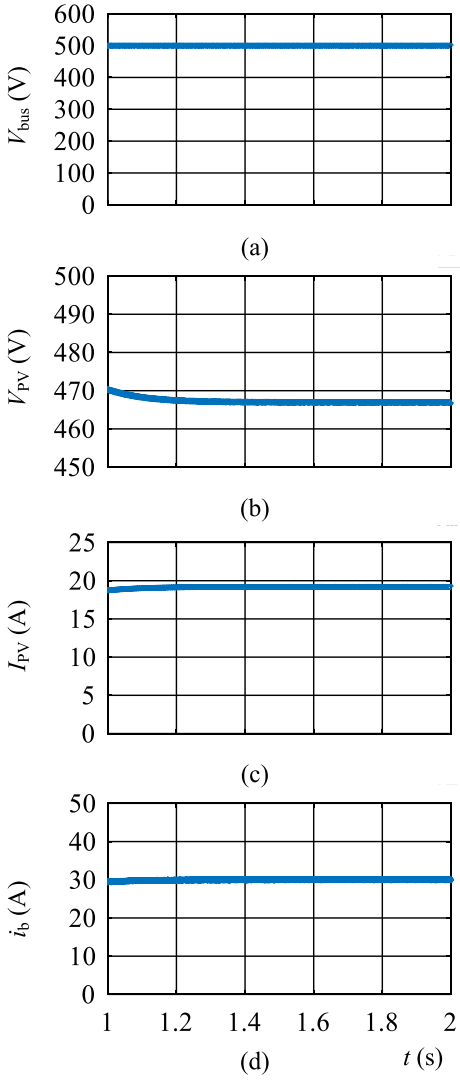

FIGURE 9. Steady state simulation results of operation scenario 5. (a) DC bus voltage V_{bus}; (b) PV voltage V_{PV}; (c) PV current I_{PV}; (d) Battery charging current i_b.

3) SCENARIO 5

The steady state simulation results of the operation scenario 5 are shown in Fig. 9. The simulation conditions are as follows: Irradiance = 1000 W/m^2, Temperature = 25 °C, the load power $P_L = 2.5$ kW. The DC bus voltage V_{bus} is controlled at the preset value $V^*_{bus} = 500$ V as shown in Fig. 9 (a). In this scenario the maximum charging current loop is enabled and the MPPT loop is disabled, and the battery charging current is controlled as $i^*_b = 30$ A, which is shown in Fig. 9 (d). From Fig. 9 (b) and Fig. 9 (c), the PV would not operate at the maximum power point in this scenario, in order to achieve the power balance of the system.

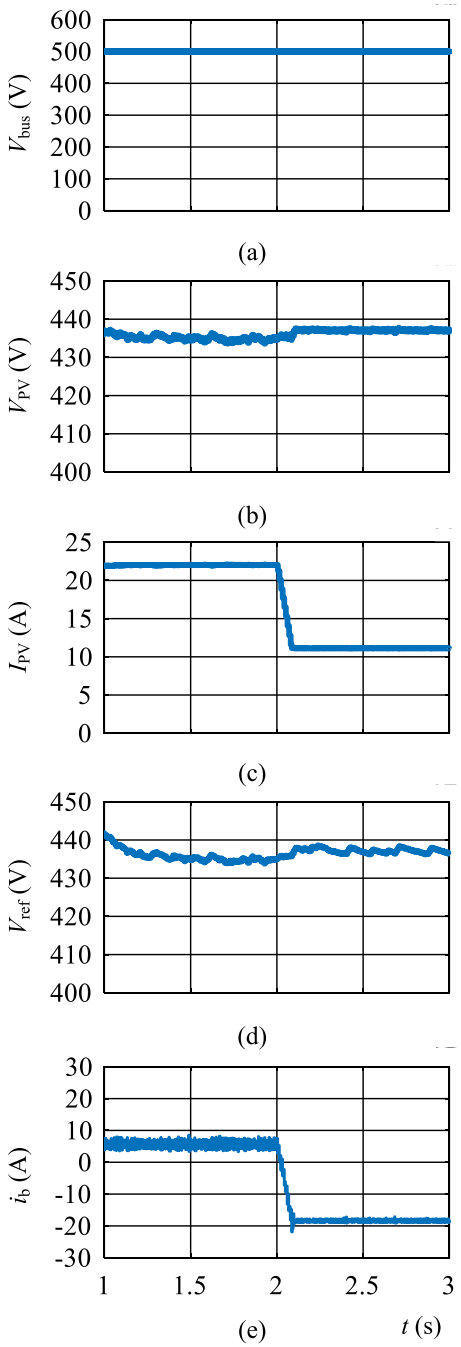

FIGURE 10. Simulation results with irradiance dropping from 1000 W/m^2 to 500 W/m^2 at $t = 2$ s. (a) DC bus voltage V_{bus}; (b) PV voltage V_{PV}; (c) PV current I_{PV}; (d) PV reference voltage V_{ref}; (e) Battery charging current i_b.

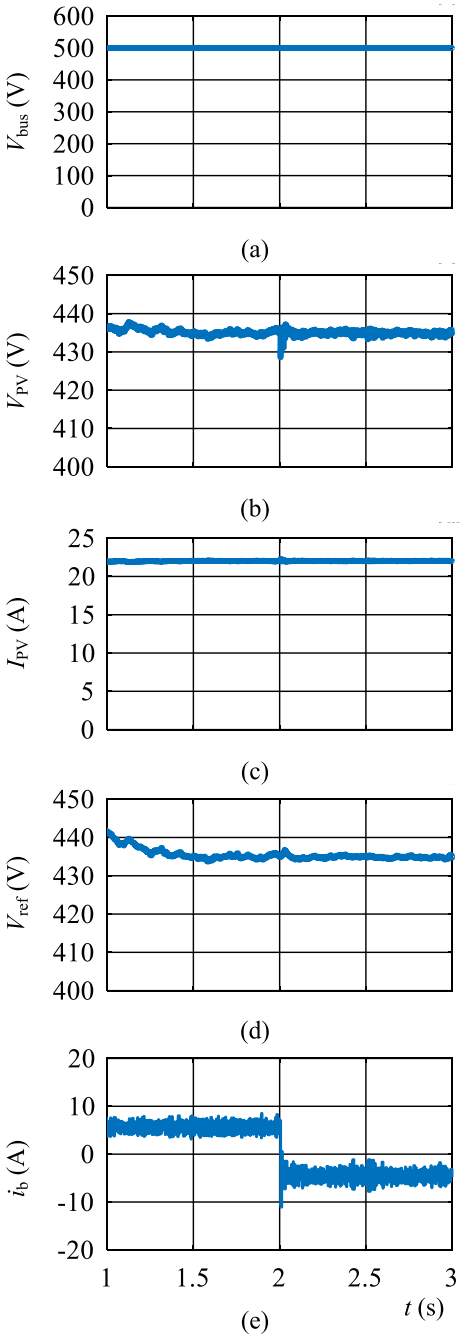

FIGURE 11. Simulation results with load power rising from 8 kW to 10 kW at $t = 2$ s. (a) DC bus voltage V_{bus}; (b) PV voltage V_{PV}; (c) PV current I_{PV}; (d) PV reference voltage V_{ref}; (e) Battery charging current i_b.

B. DYNYMIC RESPONSE SIMULATION RESULTS

1) IRRADIANCE DROPPING INCIDENT

The dynamic performance of the system with the irradiance dropping from 1000 W/m^2 to 500 W/m^2 at $t = 2$ s is presented in Fig. 10. Other simulation conditions are as follows: Temperature = 25°C, the load power $P_L = 8$ kW. The DC bus voltage V_{bus} keeps stable during the transition as shown in Fig. 10 (a). In this scenario the MPPT loop always takes charge of the control of the duty cycle D. From Fig. 10 (d), there is a slight rise of the PV reference voltage V_{ref}, due to the variation of the PV characteristic curve during the transition. From Fig. 10 (b) and Fig. 10 (c), MPPT is achieved with the PV operating near the maximum power points of the two characteristic curves. From Fig. 10 (e), the irradiance dropping incident can be considered as a transition from the scenario 4 to the scenario 2, as the battery operates in the charging mode before the transition and operates in the discharging mode after the transition.

2) LOAD RISING INCIDENT

The dynamic performance of the system with the load power P_L rising from 8 kW to 10 kW at $t = 2$ s is presented in Fig. 11. Other simulation conditions are as follows: Irradiance = 1000 W/m^2, Temperature = 25°C. The DC bus voltage V_{bus} keeps stable during the transition as shown in Fig. 11(a). In this scenario the MPPT loop is always enabled as shown from Fig. 11(b) to Fig. 11(d). Similar with the irradiance dropping incident discussed above, the load power rising incident can be considered as a transition from the operation scenario 4 to the scenario 2 as shown in Fig. 11(e).

V. CONCLUSION

An integrated three-port power converter as the interface for the PV/battery hybrid distributed power generation system is proposed. Compared with the conventional system topology containing an independent DC-DC unidirectional conversion stage and a bidirectional conversion stage, the proposed system has advantages in terms of higher power density and reliability. The phase shift angle of the full bridge and the switch duty cycle are adopted as two control variables to obtain the required DC bus voltage and realize the power balance among three ports. Different operating scenarios of the system under various power conditions are discussed in detail and a comprehensive energy management and control strategy is proposed accordingly. The priority controller can enable one of the control loops in different scenarios to optimize the whole system performance, taking both the MPPT benefit and the battery charging/discharging management requirements into consideration. The simulation results verify the performance of the proposed PV/battery hybrid distributed power generation system and the feasibility of the control algorithm.

REFERENCES

[1] F. Blaabjerg, Z. Chen, and S. B. Kjaer, "Power electronics as efficient interface in dispersed power generation systems," *IEEE Trans. Power Electron.*, vol. 19, no. 5, pp. 1184–1194, Sep. 2004.
[2] J. M. Carrasco, L. G. Franquelo, J. T. Bialasiewicz, E. Galvan, R. Potillo, M. M. Prats, J. I. Leon, and N. Moreno-Alfonso, "Power-electronic systems for the grid integration of renewable energy sources: A survey," *IEEE Trans. Ind. Electron.*, vol. 53, no. 4, pp. 1002–1016, Jun. 2006.
[3] *BP Statistical Review of World Energy*, British Petroleum, London, U.K., Jun. 2018.
[4] J. P. Barton and D. G. Infield, "Energy storage and its use with intermittent renewable energy," *IEEE Trans. Energy Convers.*, vol. 19, no. 2, pp. 441–448, Jun. 2004.
[5] M. S. Whittingham, "History, evolution, and future status of energy storage," *Proc. IEEE*, vol. 100, pp. 1518–1534, May 2012.
[6] C. A. Hill, M. C. Such, D. Chen, J. Gonzalez, and W. M. Grady, "Battery energy storage for enabling integration of distributed solar power generation," *IEEE Trans. Smart Grid*, vol. 3, no. 2, pp. 850–857, Jun. 2012.
[7] Z. Yi, W. Dong, and A. H. Etemadi, "A unified control and power management scheme for PV-battery-based hybrid microgrids for both grid-connected and islanded modes," *IEEE Trans. Smart Grid*, vol. 9, no. 6, pp. 5975–5985, Nov. 2018.
[8] H. Mahmood, D. Michaelson, and J. Jiang, "Decentralized power management of a PV/battery hybrid unit in a droop-controlled islanded microgrid," *IEEE Trans. Power Electron.*, vol. 30, no. 12, pp. 7215–7229, Dec. 2015.
[9] K. Sun, L. Zhang, Y. Xing, and J. M. Guerrero, "A distributed control strategy based on DC bus signaling for modular photovoltaic generation systems with battery energy storage," *IEEE Trans. Power Electron.*, vol. 26, no. 10, pp. 3032–3045, Oct. 2011.
[10] S. Adhikari and F. Li, "Coordinated V-f and P-Q control of solar photovoltaic generators with MPPT and battery storage in microgrids," *IEEE Trans. Smart Grid*, vol. 5, no. 3, pp. 1270–1281, May 2014.
[11] S. K. Kollimalla, M. K. Mishra, and N. L. Narasamma, "Design and analysis of novel control strategy for battery and supercapacitor storage system," *IEEE Trans. Sustain. Energy*, vol. 5, no. 4, pp. 1137–1144, Oct. 2014.
[12] S. Wen, S. Wang, G. Liu, and R. Liu, "Energy management and coordinated control strategy of PV/HESS AC microgrid during Islanded operation," *IEEE Access*, vol. 7, pp. 4432–4441, 2019.
[13] W. Jiang and B. Fahimi, "Multiport power electronic interface—Concept, modeling, and design," *IEEE Trans. Power Electron.*, vol. 26, no. 7, pp. 1890–1900, Jul. 2011.
[14] H. Krishnaswami and N. Mohan, "Three-port series-resonant DC–DC converter to interface renewable energy sources with bidirectional load and energy storage ports," *IEEE Trans. Power Electron.*, vol. 24, no. 10, pp. 2289–2297, Oct. 2009.
[15] H. Tao, J. L. Duarte, and M. A. M. Hendrix, "Three-port triple-half-bridge bidirectional converter with zero-voltage switching," *IEEE Trans. Power Electron.*, vol. 23, no. 2, pp. 782–792, Mar. 2008.
[16] Z. Qian, O. Abdel-Rahman, and I. Batarseh, "An integrated four-port DC/DC converter for renewable energy applications," *IEEE Trans. Power Electron.*, vol. 25, no. 7, pp. 1877–1887, Jul. 2010.
[17] H. Al-Atrash and I. Batarseh, "Boost-integrated phase-shift full-bridge converter for three-port interface," in *Proc. IEEE Power Electron. Spec. Conf.*, Jun. 2007, pp. 2313–2321.
[18] W. Li, J. Xiao, Y. Zhao, and X. He, "PWM plus phase angle shift (PPAS) control scheme for combined multiport DC/DC converters," *IEEE Trans. Power Electron.*, vol. 27, no. 3, pp. 1479–1489, Mar. 2012.
[19] T. Esram and P. L. Chapman, "Comparison of photovoltaic array maximum power point tracking techniques," *IEEE Trans. Energy Convers.*, vol. 22, no. 2, pp. 439–449, Jun. 2007.

JIATU HONG received the B.S. degree in electrical engineering and automation from the Dalian University of Technology, Dalian, China, in 2015, and the M.Eng. degree in electrical engineering from the Queensland University of Technology, Brisbane, Australia, in 2018. He is currently a Research Assistant with Shenzhen University, Shenzhen, China. In 2019, he will join the State Key Laboratory of Internet of Things for Smart City, University of Macau, Macau. His current research interests include high-frequency converter topology and control, and power converter in renewable generation.

JIAN YIN (M'17) received the B.Eng. degree from Shandong University, Jinan, China, in 2007, and the Ph.D. degree from The University of Hong Kong, Hong Kong, in 2015. He was an Electrical Engineer with the Grid Institute, Shandong Electric Power Engineering Consulting Institute, Jinan, China. He is currently an Assistant Professor with the College of Mechatronics and Control Engineering, Shenzhen University, Shenzhen, China. His current research interests include bidirectional converters and wireless power transfer technologies.

YITAO LIU (S'11–M'15) received the B.S. degree in electrical engineering from Wuhan University, Wuhan, China, in 2008, and the M.S. and Ph.D. degrees in electrical and electronic engineering from Nanyang Technological University (NTU), Singapore, in 2009 and 2014, respectively. From 2014 to 2015, he was a Research Fellow with the Rolls Royce-NTU Joint Laboratory. He is currently an Assistant Professor with Shenzhen University, Shenzhen, China. His current research interests include high power density converters, EMI/EMC in power electronics, and wideband-gap devices.

JIANCHUN PENG (M'04–SM'17) received the B.S. and M.S. degrees from Chongqing University, Chongqing, China, in 1986 and 1989, respectively, and the Ph.D. degree from Hunan University, Hunan, China, in 1998, all in electrical engineering. He was a Visiting Professor with Arizona State University, Tempe, AZ, USA, from 2002 to 2003, and with Brunel University, London, U.K., in 2006. He is currently a Professor with the College of Mechatronics and Control Engineering, Shenzhen University, Shenzhen, China. His current research interests include electricity markets, and power system optimal operation and control.

HUI JIANG received the B.S. degree from Chongqing University, Chongqing, China, in 1990, and the M.S. and Ph.D. degrees from Hunan University, Hunan, China, in 1999 and 2005, respectively, all in electrical engineering. From 2005 to 2006, she was a Visiting Scholar with Brunel University, London, U.K. She is currently a Professor with Shenzhen University. Her current interests include power system economics, and power system planning and operation.